

# Transfer Learning Based Screen Defect Classification

Yilei Li, Chengyuan Li, Yifan Zhang, Shuo Chang, Zixuan Wang and Fan Zhang  
{ [liyilei@bupt.edu.cn](mailto:liyilei@bupt.edu.cn), [lcyuan@bupt.edu.cn](mailto:lcyuan@bupt.edu.cn), [zhangyf@bupt.edu.cn](mailto:zhangyf@bupt.edu.cn), [changshuo@bupt.edu.cn](mailto:changshuo@bupt.edu.cn),  
[beiyouwangzi@bupt.edu.cn](mailto:beiyouwangzi@bupt.edu.cn), [zhangfan2015@bupt.edu.cn](mailto:zhangfan2015@bupt.edu.cn) }

Laboratory of Universal Wireless Communications, Ministry of Education, Beijing University of Posts and Telecommunication, Beijing, P.R.China, 100876.  
School of Information and Communication Engineering, Beijing Information Science and Technology University, Beijing, P.R.China, 100085.

**Abstract.** For the screen defect classification, human inspectors and traditional machine learning algorithms are inefficient and inaccurate. Convolutional neural network (CNN) driven by data are feasible solutions. However, real training images are limited in the industrial scenario, which causes overfitting. Hence, in this paper, a novel learning based method is proposed for defect classification, which is based on the CNN. To alleviate the problem of limited images, two strategies are introduced into model learning. For the training data, a data generation module is implemented to enlarge the training dataset. For the CNN model learning, transfer learning is applied in the whole training process. To verify the proposed method, various experiments are carried out. The results indicate that our screen defect classification model achieves superior performance.

**Keywords:** Defect Classification, Transfer Learning, CNN, Generation Module.

## 1 Introduction

In the field of industrial manufacturing, defect classification for liquid crystal display (LCD) screens is a hotspot. In general, there are different kinds of defects appearing on LCD screens [1], such as point defects, mura defects, leakage defects, etc. Some of the examples are shown in **Figure 1**.

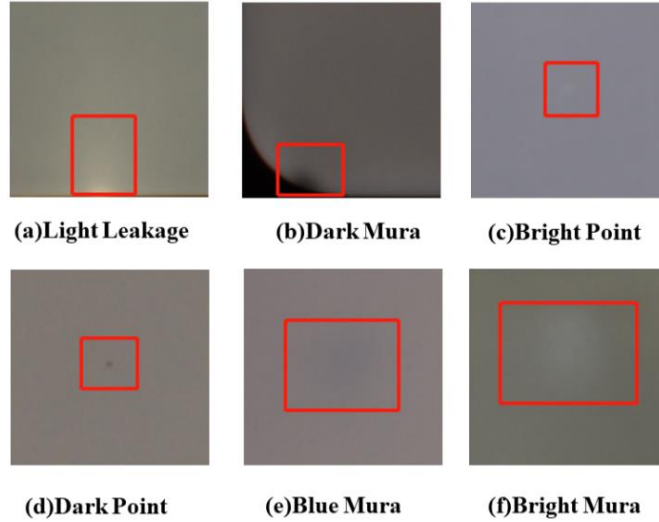


**Fig. 1.** Different screen defects.

To determine whether an LCD screen is defective or not, human inspectors are employed on the production line. But there are three drawbacks for employing human inspectors: The standards of defects are difficult to unify; The efficiency of human inspectors is low; The cost of employment is high.

Since using manual classification of screens has many disadvantages, machine learning methods are proposed [1-5]. Fundamentally, general method is mainly divided into two steps. First, the features of samples are extracted with common feature extraction algorithms, for example, HOG [4], Harr [2], and Gabor [5], etc. Second, a classification model is applied to return a final result. Generally, SVM is employed as the classification model [6][7]. However, the features extracted are not specifically designed for defect classification.

Nowadays, deep learning methods can extract features directly. However, deep learning models are data driven. In the industrial scene, the dataset is limited. Therefore, in this paper, we propose a novel method — Transfer Learning based mobile screen Defect Classification (TLDC) to tackle this issue. The framework of TLDC is depicted in **Figure 2**. With exemplar images as input, the generation module can produce many defective samples. Then, we use a data pre-processing module to exclude the backgrounds of the LCD screens and get regions of interest (ROI). Finally, the processed samples are sent to the transfer learning module to retrain a new binary classifier, where two classes are defective images and no-defective images.

Overall, TLDC is designed for industrial screen defects classification. TLDC adopts two strategies: one is the automatic generation strategy, the other is transfer learning. With the help of the generation module and transfer learning, our model is able to avoid overfitting due to insufficient data.

The main contributions of this paper are summarized as follows. A generation module is proposed. It can imitate real samples to generate similar defective samples and enlarge dataset. A pre-processing module is introduced to remove the influence of the black background.

Transfer learning is applied in our scheme when images are insufficient. Various comparative experiments are carried out to verify the effectiveness of TLDC.

The rest of the paper is organized as follows. Section 2 reviews the related work including traditional machine learning methods, deep learning models and transfer learning. The proposed TLDC approach is presented concretely in Section 3. The experimental results are given in Section 4, and finally some conclusions are drawn in Section 5.

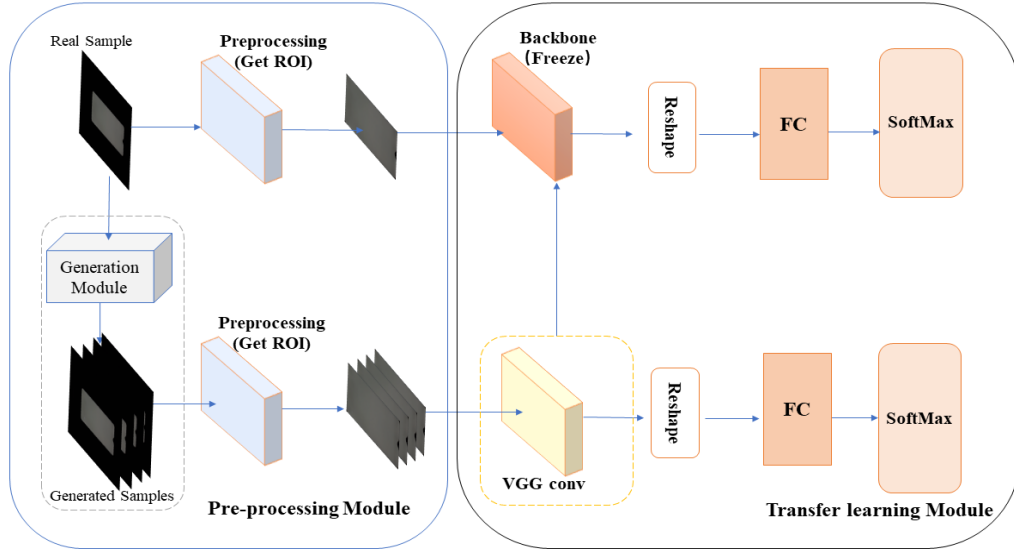


Fig. 2. The framework of TLDC.

## 2 Related Work

### 2.1 Traditional Machine Learning Methods

Harr is a traditional machine learning method for visual object classification [22], but the impact of uneven illumination in industrial manufacturing cannot be well balanced [2]. Navneet Dalal et al. proposed HOG descriptors, which can significantly outperform existing feature sets for human classification [4]. However, HOG descriptors are extremely sensitive to noise, which affects the accuracy of industrial classification [8]. Different from the HOG and Harr operator, the Gabor filter has better performance in extracting the information of the frequency domain. But it performs unstably when abrupt changes happen [5]. After feature extraction, a classifier is commonly employed to classify features, such as SVM [3]. However, SVM performs inferiorly when large-scale samples are trained.

Even though the traditional machine learning methods can accomplish defects classification in place of humans, they still has two drawbacks. First, the process of feature extraction

and classification is relatively independent. Second, its performance is unsatisfactory when the dataset is large.

## 2.2 Deep Learning Models

Deep learning methods train a multi-layer neural network model usually using massive labelled data to obtain feature maps. Specifically, deep learning methods can obtain features directly in various scenarios, for example, natural language processing (NLP) [9], medical image recognition [10], and industrial detection [11], etc. CNN is a classical deep learning model widely utilized in image classification [21] due to its superior performance and robustness [20]. Particularly, CNN consists of convolutional layer, pooling layer, and fully connected layer (FC) [12].

## 2.3 Transfer Learning

In 2013, Nitish Srivastava [13] et al. proposed a way of improving classification performance for classes which have few training examples. The key idea is to discover classes which are similar and transfer knowledge among them. Later, some researchers discovered that initializing a network with transferred features from almost any number of layers can produce a boost to generalization [14]. On the whole, transfer learning is employed for promoting the model performance in multiple tasks, such as sign language [15], face sketch recognition [16], and so on.

# 3 Model Design

The objective of our work is to judge whether an LCD screen is defective or not. Therefore, TLDC method is proposed for this purpose. The framework of the proposed transfer learning based method is shown in **Figure 2**, and the details of generation module, ROI module and transfer learning strategy are elaborated as follows.

## 3.1 Generation Module

The generation module is able to produce three types of screen defects: point, mura and line defects. Specifically, the generation principle of point and mura defects is similar. Practically, we select a point randomly in the ROI region as the center and divide the neighborhood of this center into five levels. **Figure 3** shows the definition of the neighborhood of the point defect and mura defect.

For any point in this neighborhood, its pixel value is modified according to the following steps:

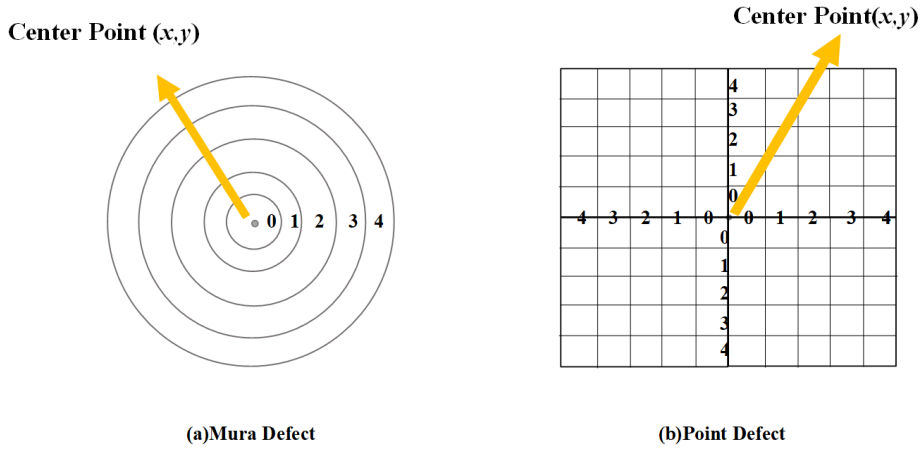


**Fig. 3.** Neighborhoods of generated defects.

First, the RGB pixel value of the center point  $(x, y)$  is calculated. Second, in the  $i$ th ( $i$  ranges from 0 to 4) level neighborhood, the pixel value in this area increases or declines by a given offset on the basis of the calculated value in the first step.

For point defects, another step is added. The image needs to be operated with linear filtering [17]. In addition, the generation of line defects varies from other types. A chosen point as the starting point of the line extends for a length in a random direction, and the pixel value of the generated line is a fixed value.

	Bright Mura	Dark Mura	Bright Point	Line
Generated Samples				
Real Samples				

**Fig. 4.** Comparisons of generated defects and real defects.

Due to the data augmentation by generation module, the limited training dataset is enlarged. **Figure 4** displays the contrast between the generated defective images and the real ones.

### 3.2 ROI Module

In order to remove the black background, we find the corner spots of the screen by the Hough transform, and then extract the ROI area of the origin image by the perspective transformation. The flowchart of the ROI module is demonstrated in **Figure 5**.

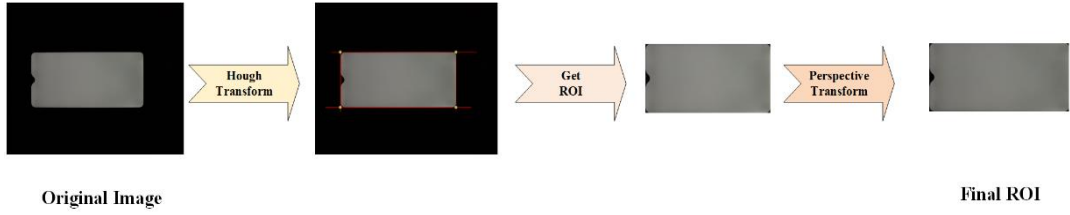


**Fig. 5.** The flowchart of getting ROI.

Next, each step in **Figure 5** is introduced separately. Hough transform is a commonly applied feature extraction technique in image processing [18]. Hough transform calculates the local maximum value of the cumulative result in  $\theta$ - $\rho$  parameter space. The principle of the Hough transform is to convert the linear equation in the Cartesian coordinate system to the linear equation in the polar coordinate system. The detailed process of the Hough transform is listed as follows. Accumulator  $H$  is initialized to all zeros. For each edge point  $(x,y)$  in the image, when  $\theta$  ranges from  $-90^\circ$  to  $180^\circ$ ,  $\rho$  and  $H(\theta, \rho)$  are calculated by the following equations:

$$\rho = x \sin \theta + y \cos \theta . \quad (1)$$

$$H(\theta, \rho) = H(\theta, \rho) + 1 . \quad (2)$$

where  $\rho$  is the distance from the straight line to the origin, and  $\theta$  is the angle between the straight line and the  $x$ -axis.

The value of  $(\theta, \rho)$  is found when  $H(\theta, \rho)$  is a local maximum. The detected line in the image is given by equation (1).

Because the LCD screens in our task are rectangular, we match four boundaries by Hough transform, and four intersections of boundary lines are the corners of the image. According to the corner information, the ROI area of the screen is obtained. Finally, the screen is projected into a fixed-size rectangular area through perspective transformation to obtain a ROI area of uniform size.

### 3.3 Transfer Learning Strategy

The transfer learning strategy has the ability to apply knowledge learned in the source domain to the target domain. In this paper, the source domain is a new dataset mixed with

generated defective images and real ones, and the target domain is a dataset which makes up of real samples. Mixed images are the input of the VGG-Net [19] to obtain a pre-trained model.

Then we transfer the feature information to the classification model with fewer samples. Specifically, the convolutional and pooling layers are transferred to the classification model. After the transfer of the convolutional and pooling layers, the classification layer needs to be reconstructed. This paper mainly retrains the FC layer of the model transferred from the source domain. Since the screen classification task is a binary classification, the parameters of the last FC layer are modified to be two. And the last FC layer is retrained. Finally, the output is passed through the SoftMax classifier as the final classification output layer. **Figure 6** illustrates the process of transfer learning in this paper.

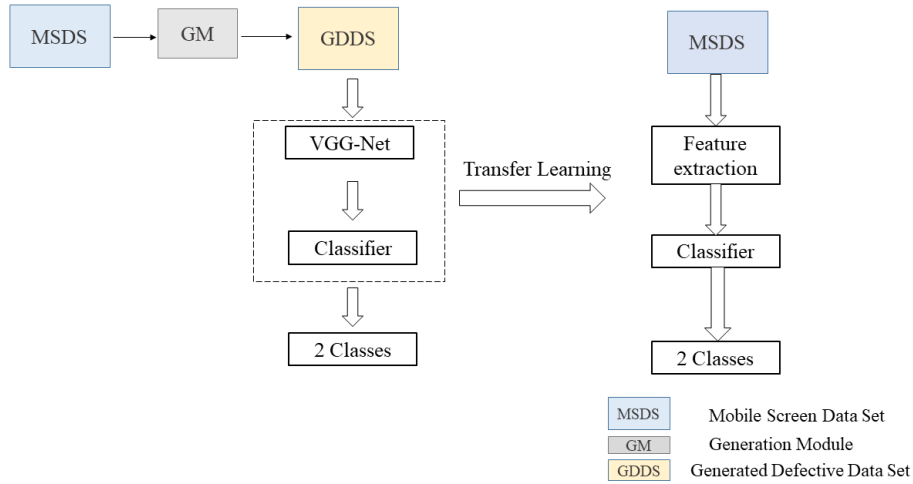


**Fig. 6.** Transfer learning in TLDC.

Besides, cross-entropy loss function is used [24]:

$$loss = -[y \log(p) + (1 - y) \log(1 - p)] . \quad (3)$$

Where  $y$  is the label of the sample, the positive class is 1 and the negative class is 0,  $p$  is the probability of the positive class.

## 4 Experiments

### 4.1 Dataset

The images used in this paper are taken by industrial cameras mounted on the production line. Each image is annotated by experienced workers. In our experiment, 168 defective images and 1032 no-defective images are collected, which is presented in Table 1.

**Table 1.** Dataset Configuration.

Images	Training Set	Valication Set	Test Set	Sum
Defective Images	860	86	86	1032
No-defective Images	140	14	14	168
Total Numbers of Set	1400	100	100	1200

## 4.2 Experimental Setup

This experiment is implemented on a Dell R7300 server with an NVidia 1080Ti GPU. All the codes in this experiment are based on the Pytorch and python3. For the algorithm optimization, the learning rate is 0.01, and the epoch is 100. TLDC is updated by stochastic gradient descent (SGD) [23].

## 4.3 Results and discussion

**Pretraining and no-pretraining.** In order to verify whether the VGG-Net based model needs pretraining, we set three models for comparison. Their accuracy on the test set is shown in Table 2. The first model in Table 2 refers to the VGG-Net with primitive parameters. The second model is pretrained with ImageNet dataset [12]. The last one is pretrained with mixed dataset. The mixed dataset consists of generated and real defective images. The pretrained VGG-Net with mixed dataset outperforms the VGG-Net about 14% on the test set. However, VGG-Net pretrained on ImageNet dataset [12] performs worse than others. In conclusion, model pretrained on a mixed dataset performs the best.

**Table 2.** Pretrain and no-pretrain.

	VGG	VGG(ILSVRC'14)	VGG(Mixed Dataset)
Accuracy( <b>test</b> )	83%	73%	97%

**The mixing ratio.** The comparison results of different mixing ratios are presented in **Figure 7**. It can be seen that when the mixing ratio of real to generated images is 1:15, model performs best. Note that, while the proportion of real samples is too high or too low, the accuracy of the model declines. Hence, we can conclude that dataset with appropriate mixing rate can help models gain improvement.



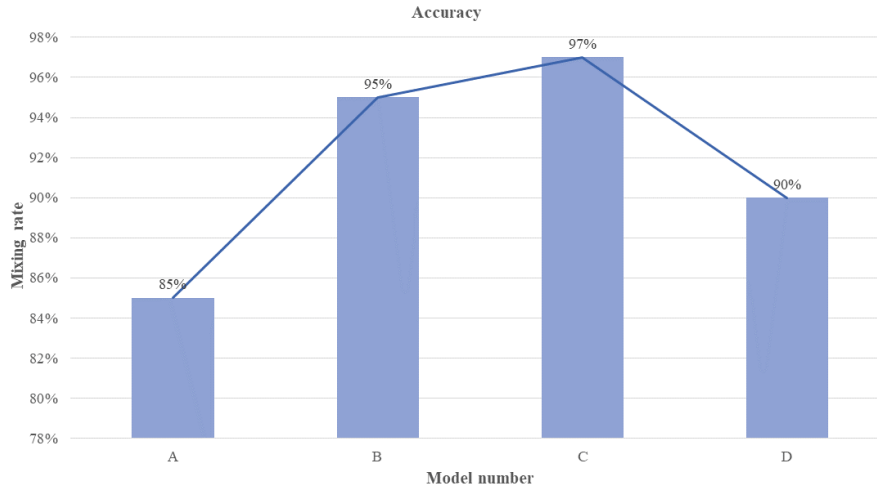


**Fig. 7.** Accuracy of different mixing ratios. From left to right, the mixing ratios of the real images to the generated ones are 0:1, 1:20, 1:15, 1:10.

In summary, selecting a mixture of real and generated samples of appropriate proportions for transfer learning can help model achieve high accuracy in industrial tasks.

## 5 Conclusion

In this paper, a new data generation strategy and transfer learning strategy have been introduced for defect classification. Compared with other machine learning methods, our method can solve the issue of limited dataset and learn from domain knowledge. In view of proposed methods, our classifier achieves optimal performance. Although this paper focused on screen defects, the methods mentioned in this paper can be carried out in other similar tasks. In future work, the problem of industrial classification and complex scenes will be further explored.

**Acknowledgments.** This work was supported in part by the National Natural Science Foundation of China under Grant (61801052), in part by the National Key Research and Development Program of China under Grant (2019YFB1804400, 2018YFF0301202), and in part by the Beijing Natural Science Foundation under Grants (4202046).

## References

- [1] J. Y. Lee and S. I. Yoo: Automatic Detection of Region-mura Defect in TFT-LCD. IEICE Transactions on Information and Systems. pp. 2371-2378 (2004)
- [2] P. Viola, M. Jones et al.: Rapid Object Detection Using a Boosted Cascade of Simple Features. Vol. 1, pp. 511-518. IEEE Conference on Computer Vision and Pattern Recognition. USA (2001)

- [3] P.-H. Chen, A.: A Tutorial on  $\nu$ -support Vector Machines. *Applied Stochastic Models in Business and Industry*. pp. 111-136 (2005)
- [4] N. Dalal, C.-J. Lin, and B. Scholkopf: Histograms of Oriented Gradients for Human Detection. Vol. 1, pp. 886-893. *IEEE Conference on Computer Vision and Pattern Recognition*. USA (2005)
- [5] Z. Liu, Q. Hu, J. Liu, and B. Zhang: Stereo Matching Using Gabor Convolutional Neural Network. *International Workshop on Human Friendly Robotics*. pp. 48-53 (2018)
- [6] D. F. Llorca, R. Arroyo, and M.-A. Sotelo: Vehicle Logo Recognition in Traffic Images Using HOG Features and SVM. *IEEE Conference on Intelligent Transportation Systems*. pp.2229-2234 (2013)
- [7] E. Gao, Q. Gao, and J. Chen: The Welding Region Extraction Technology Based on HOG and SVM. *International Conference on Education, Management, Computer and Society*. pp. 2371-2378 (2004)
- [8] S. Ramezani and R. P. R. Hasanzadeh: Defect detection in metallic structures through AMR C-scan images using deep learning method. *International Conference on Pattern Recognition and Image Analysis*. pp. 135-140 (2019)
- [9] W. Yin, K. Kann, M. Yu, and H. Schutze: Comparative Study of CNN and RNN for Natural Language Processing. *arXiv preprint arXiv:1702.01923*, 2014
- [10] L. Li, J. Wu, and X.Jin: CNN Denoising for Medical Image Based on Wavelet Domain. *International Conference on Information Technology in Medicine and Education*. pp. 105-109 (2018)
- [11] M. Canizo, I. Triguero, A. Conde, and E. Onieva: Multi-head CNN--RNN for Multi-time Series Anomaly Detection: An Industrial Case Study. *Neurocomputing*. pp. 246-260 (2019)
- [12] A. Krizhevsky, I. Sutskever, and G. E. Hinton: Imagenet Classification with Deep Convolutional Neural Networks. *Advances in Neural Information Processing Systems* 25. pp. 1097-1105 (2012)
- [13] N. Srivastava and R. R. Salakhutdinov: Discriminative Transfer Learning with Tree-based Priors. *Advances in Neural Information Processing Systems* 27. pp. 3320-3328 (2014)
- [14] J. Yosinski, J. Clune, Y. Bengio, and H. Lipson: How Transferable Are Features in Deep Neural Networks? *IEICE Transactions on Information and Systems*. pp. 2371-2378 (2004)
- [15] A. Farhadi, D. Forsyth, and R. White: Transfer Learning in Sign Language. *IEEE Conference on Computer Vision and Pattern Recognition*. pp. 1-10 (2019)vol.31.
- [16] W. Wan, Y. Gao, and H. J. Lee: Transfer Deep Feature Learning for Face Sketch Recognition. *Neural Computing and Applications*. pp. 1-8 (2007)
- [17] R. Shapiro: Linear Filtering. *Mathematics of computation*. pp. 1094-1097 (1975)
- [18] A. M. Nickfarjam, H. Ebrahimpour-komleh, and A. A. A. Tehrani: Binary image matching using scale invariant feature and hough transforms. *Advances in Science and Engineering Technology International Conferences*. pp. 1-5 (2018)
- [19] K. Simonyan and A. Zisserman: Very Deep Convolutional Networks for Large-scale Image Recognition. *arXiv preprint arXiv:1409.1556*, 2014
- [20] S. Huang, Y. Jiang, Y. Gao et al: Automatic Modulation Classification Using Contrastive Fully Convolutional Network. *IEEE Wireless Communications Letters*. pp. 1044-1047
- [21] S. Huang, Y. Jiang, X. Qin et al.: Automatic Modulation Classification of Overlapped Sources Using Multi-Gene Genetic Programming With Structural Risk Minimization Principle. *IEEE Access*. pp. 48827-48839 (2018)
- [22] S. Huang, Y. YuanYuan, W. Zhiqing et al.: Automatic Modulation Classification of Overlapped Sources Using Multiple Cumulants. *IEEE Transactions on Vehicular Technology*. pp. 6089-6101 (2017)
- [23] L. Bottou: Stochastic gradient descent tricks. *Neural networks: Tricks of the trade*. pp. 421-436 (2012)

- [24] P.-T. De Boer, A.: A tutorial on the cross-entropy method. *Annals of operations research*. pp. 19-67 (2005)